DOI 10.1007/s11106-017-9843-2
Powder Metallurgy and Metal Ceramics, Vol. 55, Nos. 9-10, January, 2017 (Russian Original Vol. 55, Nos. 9-10, Sept.-Oct., 2016)

ELECTRODE MATERIALS FOR COMPOSITE AND MULTILAYER ELECTROSPARK-DEPOSITED COATINGS FROM Ni–Cr AND WC–Co ALLOYS AND METALS

V. B. Tarelnyk,[1] A. V. Paustovskii,[2] Yu. G. Tkachenko,[2,4] E. V. Konoplianchenko,[1] V. S. Martsynkovskyi, [1] and B. Antoszewski[3]

UDC 621.762:9.048.4:621.788

The layer-by-layer electrospark deposition of Cu, In, Pb, Cd, and Sn group metals and Ti, V, and W metals, as well as their carbides and hardmetals of WC type, onto metallic surfaces is studied. This technique improves the quality and wear resistance of the surface layer compared to coatings without a sublayer. The sintered electrode materials containing 10–30 wt.% of the (Ni–Cr–Si–B)–WC6 alloy allow electrospark coatings with thickness up to 100 μm and microhardness 12.3–14.2 GPa to be formed. The wear resistance and service life of these coatings are substantially higher than of those made of standard hardmetal WC6. Among the Ni–Cr–Al alloys, the best effectiveness in worn-part recovery is shown by the alloy from the ternary eutectic region (50.3 wt.% Ni, 40.2 wt.% Cr, 9.5 wt.% Al), which may provide coating thickness up to 1.0 mm. The novel coating technique and proposed electrode materials increase the resistance of cutting tools and life of equipment parts.

Keywords: *electrospark deposition, electrode materials, erosion properties, coating properties, wear resistance, multilayer coatings.*

INTRODUCTION. STATE-OF-THE-ART. PROBLEM STATEMENT

Advances in the electrospark deposition of coatings onto metallic surfaces are largely associated with extensive research efforts conducted to ascertain what effect the phase composition and structure of electrode materials have on the material mass transfer and coating properties. A spark discharge occurs in microscopic volumes and lasts 50–400 msec. These processes involve high energy fluxes, influencing the electrode (anode) erosion and transfer and the properties of coatings formed on the cathode. The study of these phenomena has underlain a series of materials science solutions related to the electrospark deposition of coatings with desired properties.

The electrode materials are currently developed in several areas. One is to improve the composition and structure of hardmetals (primarily those made of tungsten and titanium carbides) using complex metallic binders and ultrafine starting powder mixtures and employing advanced consolidation techniques [1, 2]. The other area is to

[1]Sumy National Agrarian University, Sumy, Ukraine. [2]Frantsevich Institute for Problems of Materials Science, National Academy of Sciences of Ukraine, Kiev, Ukraine. [3]Kielce University of Technology, Kielce, Poland.

[4]To whom correspondence should be addressed; e-mail: tkachenko_yuri@ukr.net.

Translated from Poroshkovaya Metallurgiya, Vol. 55, Nos. 9–10 (511), pp. 100–115, 2016. Original article submitted February 21, 2016.

produce electrode materials from metallic alloys and intermetallide-hardened materials [3, 4]. Refractory alloy systems are used as well [5, 6].

The layer-by-layer electrospark deposition of metals and refractory compounds or hardmetals onto metallic surfaces is a very promising technique. To increase the wear resistance of a copper electrode in welding of galvanized steel sheets, a three-layer (TiC–Ni)–Ni coating with a Ni sublayer was deposited onto the electrode [7]; there is also experience in applying multilayer coatings onto titanium alloy VT3-1 [8].

In general, our previous research efforts [9] showed that the electrode materials for wear-resistant coatings should have heterogeneous structure. One of the options for this structure is a eutectic consisting of metal-based solid solutions (featuring high solubility in the substrate) and hard phases. These are Ni–Cr–Al alloys, whose phase composition corresponds to a ternary eutectic of α-Cr, γ-Ni, and β-Ni–Al solid solutions.

The alloys based on Ni–Cr and other additions, such as Si, B, Fe, W, and Mo, are used to protect steel parts by slurry welding, spraying, and coating [10–12]. This increases the hardness, wear resistance, and corrosion resistance. Note that the coatings produced by these methods have not found wide application because of poor adhesion to the substrate. The γ-Ni oversaturated solid solution is the main structural phase of alloy coatings, and chromium and nickel borides of variable composition are hardening phases. Boron and silicon form low-melting eutectics with melting points of 950–1080°C and reduce oxide films on the substrate with borosilicate slurries emerging in the presence of a liquid phase (self-fluxing) and improving substrate wetting with the molten metal. This all confirms that the Ni–Cr–B–Si alloy is beneficial as electrode material for electrospark deposition.

Our studies, in particular [13], show that electrospark deposition of carbides, metals, or hardmetals onto a steel substrate with a Cu, In, Sn, Cd, or Pb sublayer increases the wear resistance of coatings by three to six times compared to the same coating without a sublayer, though the surface microhardness decreases substantially. When a second layer is applied, the initially deposited layer of low-melting metal dissolves and fills microirregularities and pores of the base coating. The second layer crystallizes more slowly since the heat is removed by the liquid low-melting metal. The surface roughness reduces to R_a = 0.6–0.8 μm. The microhardness of the electrospark-deposited composite coating significantly depends on the amount of the soft, lower-melting metal in the sublayer. We previously found that copper exhibited the most stable mass transfer to metallic surfaces among all metals. We also studied how the copper content of the composite coating influenced the surface layer microhardness [14].

In the above regard, we identified the following objectives for our research:

- produce electrode materials from the Ni–Cr–Al and Ni–Cr–Si–B systems and WC–Co hardmetals for electrospark deposition and recovery of worn parts;
- establish patterns of the electrospark deposition of coatings, including that with alternating deposition electrodes for layer-by-layer deposition of various metals, alloys, and WC–Co hardmetal onto the substrate and examine properties of the coatings;
- assess effectiveness of the materials and technique for electrospark deposition and recovery of worn parts in industrial conditions (in particular, for restoration of worn shaft necks and bearing seats in electric motor bodies, where the coating is required to have a thickness to 1 mm and adequate hardness, and for hardening of compressor blades to improve their resistance to gas abrasive wear).

EXPERIMENTAL PROCEDURE

As the base composition for the Ni–Cr–Al samples, we selected the alloy consisting of 50.3 wt.% Ni, 40.2 wt.% Cr, and 9.5 wt.% Al. This alloy (henceforth, alloy 4A) falls into the ternary eutectic region, including solid solutions based on nickel, chromium, and chromium-doped nickel intermetallide. Alloy 4A was produced by three different techniques: arc melting, dynamic hot pressing, and vacuum sintering of powder mixtures. For sintering of alloy 4A, the charge material was a powder mixture of nickel (PNE-1 grade) and chromium (PKhM) with 40 μm particles, Ni–Al aluminide (PN70Yu30) with 50 μm particles, and aluminum (PAP-91) with particles smaller than 10 μm in ratios corresponding to the nickel, chromium, and aluminum contents of as-cast alloy 4A. We obtained mixtures of three compositions with different chromium and nickel ratios (henceforth, 4AS1, 4AS2, and 4AS3). The percentage of elements in the sintered alloys is shown in Table 1.

TABLE 1. Charge Composition for Ni–Cr–Al Alloys

Alloy	Content of elements, wt.%			
	Ni	Cr	Al	NiAl
4A	50.3	40.2	9.5	–
4AS1	33	41	–	26
4AS2	39	35	–	26
4AS3	32	40	2	26

TABLE 2. Weight Increment of Copper-Doped Steel 45 Samples

Capacitance C, μF	Short-circuit current J_{sc}, A	Discharge energy W_u, J	Cu weight increment, mg/cm^2
20	0.2–0.4	0.01	2.85
20	0.5–0.6	0.02	5.13
300	1.6–2.0	0.24	11.53
300	2.0–2.2	0.42	15.63

The samples were sintered in two stages. They were preliminary sintered in a muffle furnace in hydrogen at about 800°C for 2 h with temperature being increased at 0.06°C/sec. The samples were placed into a steel crucible filled with calcined alumina including 32% of graphite chips. The samples were finally sintered in a vacuum furnace at $6.66 \cdot 10^{-3}$ Pa and 1070°C—which is $0.8T_{melt}$ of the Ni–Cr–Al alloy (1240°C). The samples sintered in this way had no more than 12% porosity. A DRON-3M diffractometer with filtered K_α-Cu radiation was employed for X-ray diffraction.

Mixture 1M (70 wt.% Ni, 20 wt.% Cr, 5 wt.% Si, and 5 wt.% B) was prepared from Ni, Cr, Si, and B powders with particles no greater than 40 μm. The powders were dried in air ovens at 150–200°C and sieved through a 0075 mesh screen. The WC6 hardmetal mixture was dried in vacuum at 150°C and sieved through a 0075 mesh screen. Then the hardmetal and self-fluxing mixtures were loaded into a stirring machine in the ratios such as 100% 1M, 50% WC6–50% 1M, 60% WC6–40% 1M, 70% WC6–30% 1M, 80% WC6–20% 1M, 90% WC6–10% 1M, and 100% WC6, and further subjected to common dry mechanical mixing for 24 h. The mixtures were blended with a plasticizing agent (5% solution of chemical rubber in benzene). Samples of required sizes were compacted in metallic dies at 70–100 MPa and sintered at 1400–1500ºC in hydrogen. The resultant electrodes were used for electrospark deposition of coatings onto steels 45 and R6M5 (UILV-8 unit, mode 5, discharge energy W_u = = 0.42 J). Preliminary indium and copper layers were deposited in modes 2 and 3, respectively, employing the same unit at W_u = 0.015 and 0.02 J and deposition time T = 5 and 4 min/cm^2.

To develop coatings for protection of rotor wheels of centrifugal compressors against gas abrasive wear, the coatings on 100 mm × 50 mm × 6 mm sheet steel 30KhGS samples were tested in laboratory for wear resistance in a gas abrasive jet. The samples were tested in sandblasting chambers connected to air piping with 600 kN/m^2 pressure. The abrasive was quartz sand with particles 0.2 mm in diameter. The samples were placed under the nozzle on special stands at incidence angles of 90 and 45°. For comparison, we tested the coated samples (three samples per series) and uncoated reference samples made from heat-treated steel 30KhGS with hardness HB = 296–302. The wear resistance of the samples was evaluated from weight loss.

To ascertain the effect of copper amount in the composite coatings on the structure and microhardness, copper was deposited in different UILV-8 modes onto 10 mm × 10 mm × 10 mm steel 45 samples heat-treated to reach hardness 2.8 GPa. The deposition time was 1 min/cm^2. The mass transfer kinetics was studied by gravimetry with an accuracy of 10^{-5} g. The experimental results are summarized in Table 2.

Hardmetal WC8 was deposited as the second layer onto all samples in mode 5 at $W_u \approx 0.42$ J and $T = 1$ min/cm^2. Then the roughness of the coatings was measured with a surface roughness recorder/meter (model 201, Caliber Factory), and metallographic analysis was carried out with a Neophot-2 optical microscope. The microhardness across the surface layer was measured with a PMT-3 meter using a diamond pyramid under a load of 0.5 N.

The wear resistance of metal-cutting tools (high-speed steel R6M5) hardened by electrospark coatings deposited with electrodes made of hardmetal WC6 and alloy 1M in different ratios was examined in industrial environment.

EXPERIMENTAL RESULTS AND DISCUSSION

Electrode Materials and Coatings from Ni–Cr–Al Alloys. The nickel alloys conventionally include basic doping elements, chromium and aluminum, leading to the formation of a hardening phase in the Ni–Cr–Al system, representing chromium-doped nickel aluminides that ensure high strength and oxidation resistance of the alloys. The main condition for developing alloys in this system for electrospark deposition of coatings onto structural steels is the presence of eutectic structures containing both solid solutions based on metals with high solubility in the doped substrate (iron) and intermetallic phases (NiAl, Ni_3Al, and Ni_2Al_3) with high hardness. Further use of such electrodes ensures coatings with heterophase structure, featuring strong adhesion to the substrate, wear resistance, and oxidation resistance.

We examined the structure and phase composition of the Ni–Cr–Al electrode materials depending on the production technique. The microstructures of the alloys in different states are shown in Fig. 1.

The microstructure of the as-cast alloy represents a ternary eutectic (Fig. 1*a*) and that of the hot-pressed and sintered alloys (Fig. 1*b*, *c*) is a grain mixture of the α-Cr, γ-Ni, and β-NiAl solid solutions. X-ray diffraction shows that the fcc lattice parameter of the γ-Ni solid solution reaches 0.3582 nm, exceeding the nickel lattice parameter (0.3520 nm). This testifies that nickel dissolves chromium and aluminum with greater atomic radii ($r_{Cr} = 0.128$ nm and $r_{Al} = 0.143$ nm versus $r_{Ni} = 0.124$ nm).

The bcc lattice parameter of the α-Cr solid solution reaches 0.2895 nm (although it dissolves nickel having a smaller atomic radius than chromium) since aluminum is more soluble in chromium than in nickel. The bcc lattice parameter of nickel aluminide is 0.2879 nm.

The kinetic dependences of anode erosion Δ_a and cathode increment Δ_c for the Ni–Cr–Al alloys were examined during electrospark deposition of sintered alloys onto the steel substrate for 10 min using an EFI-46A unit (Fig. 2). Erosion of the sintered alloys (Fig. 2*a*, *b*) is two to four times higher than that of as-cast and hot-pressed 4A (Fig. 2*c*, *d*). The weight increment of the sintered alloy cathode (4AS2) differs little from that of the as-cast and hot-pressed alloy cathode (4A). In our case, the electrodes have the same elemental composition but different structural features (Fig. 1), resulting from their production technique. Erosion of the electrodes differs because of the distinct starting microstructure and porosity.

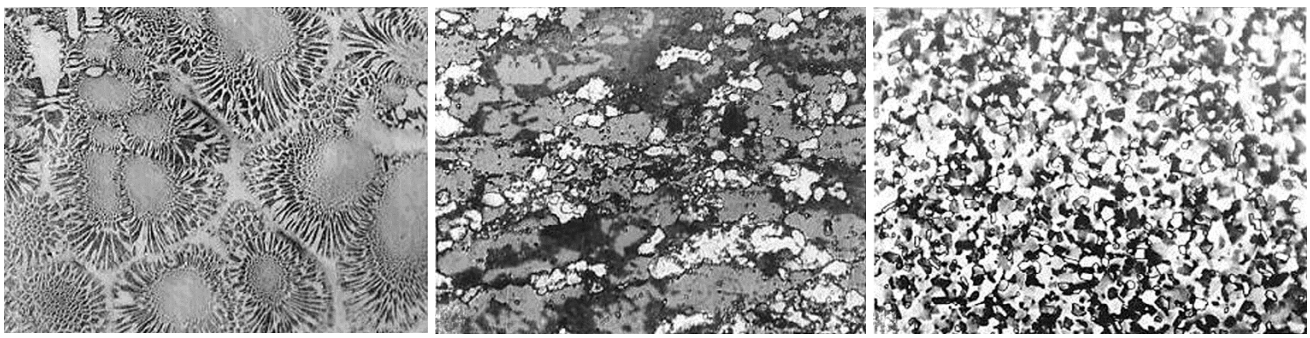

a *b* *c*

Fig. 1. Microstructures of as-cast (*a*) and hot-pressed (*b*) alloy 4A and sintered alloy 4AS3 (*c*); ×500

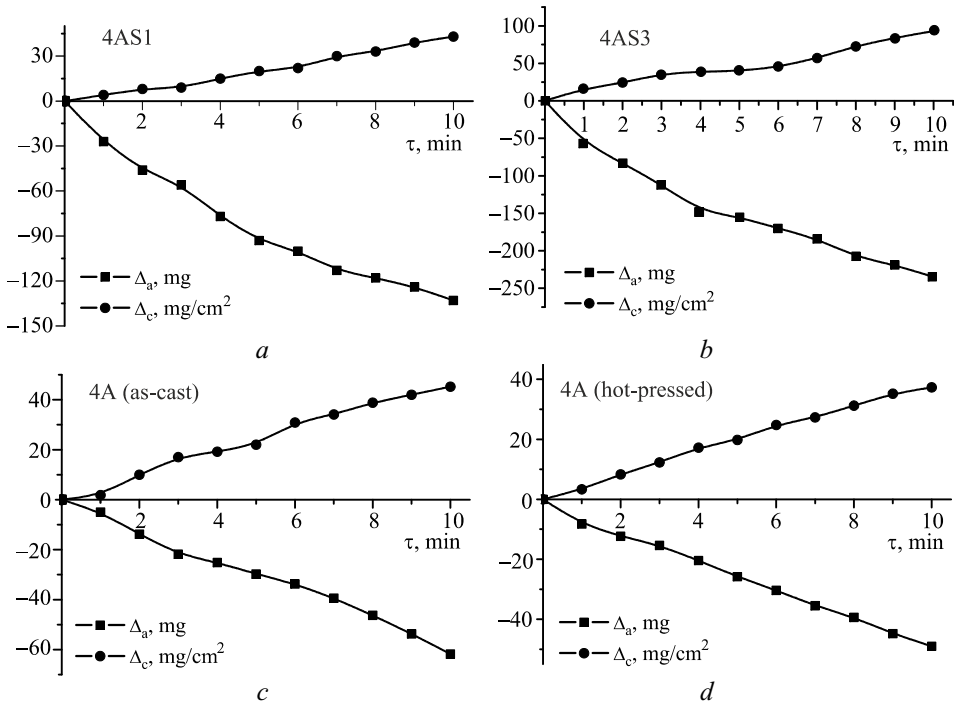

Fig. 2. Kinetic dependences of anode erosion Δ_a and cathode weight increment Δ_c in electrospark deposition of different alloys on steel 45

High erosion of the sintered alloys is attributed to weak bonds between individual structural fragments, resulting in greater destruction under a spark pulse. Depending on electrode composition and production technique, the transfer coefficient Δ_c/Δ_a varies from 0.2 for alloy 4AS1 to 0.8 for as-cast and hot-pressed 4A. The monotonous weight increment of the cathode in the deposition process indicates that the surface layer has not reached the brittle fracture threshold for 10 min deposition. The surface layer thickness (0.7–1.0 mm) allows this material to be recommended for the recovery of worn parts. Coatings from the as-cast and hot-pressed alloys are characterized by high integrity. The microhardness of the as-cast alloy coatings reaches 8–9 GPa, that of the hot-pressed coatings is 7.5–8.8 GPa, and that of the sintered ones is 7.2–8.8 GPa.

Analysis of the microstructure and wear resistance of the alloys and kinetics of electrospark deposition using Ni–Cr–Al alloy electrodes has shown that alloy 4A from the ternary eutectic region (50.3 wt.% Ni, 40.2 Cr, 9.5 wt.% Al) is the most effective for recovery of worn parts. This alloy was applied to samples from steels 35, 45, and 30KhGSA and to alloys ZhS6K and VT-22. The coating can reach 1.0 mm in thickness with use of an ELITRON-52 unit in mode 0 (W_u = 7.5 J). The results of tests for wear resistance in dry friction conditions are summarized in Table 3. The highest wear resistance is shown by electrode 4A. As is seen, the alloy 4A electrode produces coatings with wear resistance being 2.8–3.5 times higher than that of the substrates.

The Ni–Cr–Al alloy electrode was used in industrial conditions at the *Ukrmetallurgremont* Enterprise (town of Kamenskoe) for electrospark deposition of coatings to restore seating surfaces for overhead crane crabs and seating surfaces for bearings in motor covers.

Electrode Materials and Coatings from (Ni–Cr–SiB)–WC6. Some properties of the electrospark-deposited coatings on steels 45 and R6M5 produced with sintered WC6–1M (Ni–Cr–Si–B) electrodes are summarized in Table 4.

The experiments show that the electrodes containing 10–30 wt.% 1M and hardmetal WC6 produce the surface layer with microhardness 12.3–14.2 GPa. The indium sublayer decreases roughness of the 10% 1M–WC6 coating from R_a = 3.5–4.2 to R_a = 0.6–0.9 μm and increases the integrity from 80 to 90%, but reduces the microhardness to 13.25 GPa. Alloy 1M permits coatings with thickness to 75 μm and microhardness to 8.35 GPa.

TABLE 3. Wear Resistance of Uncoated Steels and Steels with Electrospark-Deposited Coatings from As-Cast Alloy 4A

Surface type	Hardness *HRC*	Wear rate *I*, μm/km	Friction coefficient *f*
Alloy 4A	60	4.7	0.32
Steel 35	31	43.3	0.34
Coating on steel 35	45	14.2	0.33
Steel 45	32	39.5	0.31
Coating on steel 45	44	13.9	0.32
30KhGSA	38	34.6	0.30
Coating on 30KhGSA	43	12.9	0.31
ZhS6K	50	7.3	0.30
Coating on ZhS6K	52	5.6	0.32
VT-22	21	70.4	0.40
Coating on VT-22	36	20.3	0.35

TABLE 4. Properties of Electrospark-Deposited Coatings Containing Alloys 1M (Ni–Cr–Si–B) and WC6

Coating material, wt.%	Layer thickness, μm	Microhardness H_μ, GPa	Integrity, %
Steel 45			
WC6–50 1M	5–50	8.9	75
WC6–40 1M	5–45	11.5	75
WC6–30 1M	10–40	12.3	75
WC6–20 1M	10–40	13.25	80
WC6–10 1M	10–40	14.2	80
WC6	10–30	12.5	80
1M	40–75	8.35	60
Cu–1M	20–25	6.03	85
In–(WC6–10 1M)	15–20	13.25	90
R6M5			
1M	50–75	11.5	90
WC6–50 1M	40–50	12.0	70
WC6–40 1M	30–40	12.5	75
WC6–30 1M	25–35	13.0	80
WC6–20 1M	25–35	13.5	80
WC6–10 1M	20–30	14.2	85
In–1M	10–15	12.25	90
In–(WC6–10 1M)	15–20	13.25	90

Figure 3 shows cross-sections of the coatings on steel 45. The cross-sections indicate that the coatings primarily represent a porousless layer from 25 to 75 μm in thickness depending on composition. There are sometimes chains of small pores, including layers adjacent to the steel substrate (this layer is dark in the figures). There are also regions without a sublayer (Fig. 3*a*–*c*), especially in case of indium (Fig. 3*d*). The microhardness of all coatings increases closer to the surface.

Data on the gas abrasive wear of steel 30KhGSA samples with and without coatings from alloys 1M and 1M-WC6, as well as standard hardmetals WC6 and T15K6, in sandblasting chambers are summarized in Table 5. The samples were hardened employing a UILV-8 unit with a manual vibrator at $W_u = 0.42$ J and $T = 1$ min/cm^2.

The tests show that the samples made of steel 30KhGSA with WC6–10% 1M coating have erosion wear resistance higher by 3.5 times than the uncoated samples and higher by 1.9, 1.5, and 1.7 times than the samples

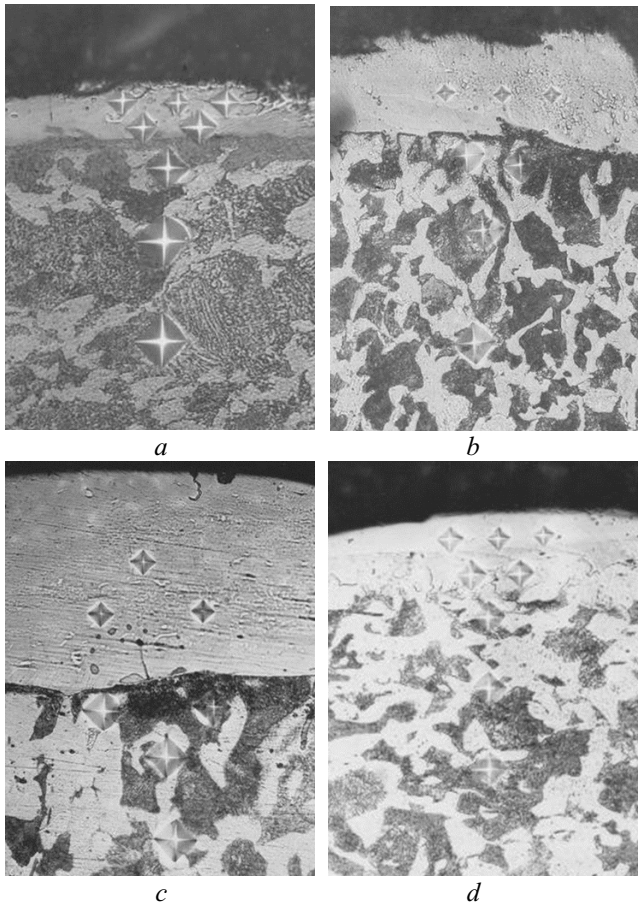

Fig. 3. Cross-sections of electrospark-deposited coatings from *a*) WC6–40% 1M, *b*) WC6–20% 1M, *c*) 1M, and *d*) In–(WC6–10% 1M) electrodes on steel 45; ×400

hardened with alloys WC6, T15K6, and 1M, respectively. The wear resistance of the samples located at an incidence angle of 90º is greater than that of the samples located at 45°.

The coatings produced with the WC6–1M electrodes have found application at the Severodonetsk Association *Azot* for repair of a Hitachi 2MCL-456 air compressor (Japan). The complexity and high production cost of centrifugal compressor rotor wheels necessitate their lifetime extension. In most cases, rotor wheels fail

TABLE 5. Results from Comparative Tests for Gas Abrasive Wear of Steel 30KhGSA Samples with and without Coatings

Coating material, %	Weight loss, g	Testing time, h	Incidence angle, grad
Uncoated	51	1	45
Uncoated	38	1	90
WC6	29	1	45
WC6	21	1	90
T15K6	23	1	45
T15K6	17	1	90
1M	27	1	45
1M	20	1	90
WC6 + 10 1M	16	1	45
WC6 + 10 1M	11	1	90

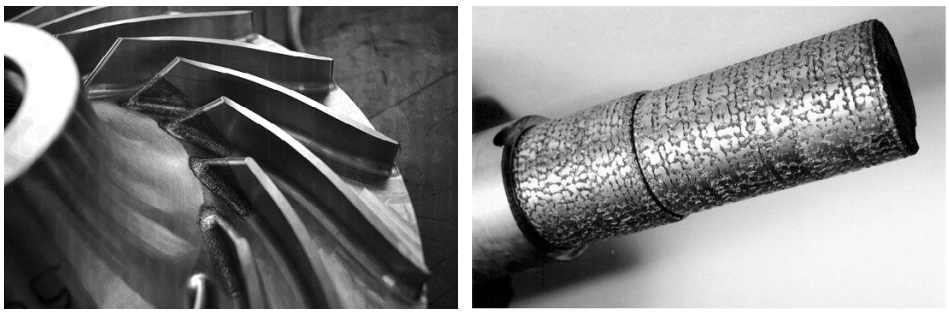

a *b*

Fig. 4. Compressor rotor wheel after electrospark hardening (*a*) and engine rotor shaft neck after electrospark size recovery (*b*)

because of gas abrasive wear of the blade roots. This is associated with the wheel performance conditions: atmospheric air containing abrasive particles, 100% relative humidity, 0.7 MPa pressure at inlet of the first rotor wheel, 10,500 rpm rotor frequency, and 258 m/sec rotary velocity. Colliding with the wheel blade leading edge, abrasive particles break off metal particles from the blade surface layer leaving caverns, which develop with time and lead to extensive metal removal with the resulting streams and slits. There are cases when the rotor wheel completely cut off and led to severe accidents. Even insignificant blade wear seriously affects the compressor's performance, and further wear causes its complete stop.

Wear-resistant coating was deposited onto leading edges and adjacent parts of rotor wheel blades (Fig. 4*a*). The electrode was WC8–10% 1M composite promoting high resistance to gas abrasive wear. The coating thickness was 80–100 μm and microhardness 14.0 GPa (substrate hardness being 4.0 GPa); this allowed blade resistance to be increased and maintenance cost to be reduced. The total annual economic effect from this novel technique has already reached 27,000 UAH only for one compressor.

To find the optimum coating material for metal-cutting tools, the Sumy Machine Building Association tested steel R6M5 end mills (36 mm in diameter) by cutting groves in rotor wheel disks made of steel 09KhA15N8Yu employing a numerically controlled 654F3 machine. The mills were hardened using a UILV-8 unit at W_p = 0.42 J. Note that the mill can process a fractional number of disks on one rotor wheel until it dulls as this involves great milling volume. The testing results show (Table 6) that the WC6–10% 1M composite electrodes used for hardening of mills significantly increase their resistance, being more than twice higher than that of the mills coated with alloy WC6.

TABLE 6. Results from Comparative Industrial Resistance Tests of End Mills in Steel 09KhA15N8Yu Processing

Electrode material, %	Number of processed parts	Resistance improvement factor
–	1.0	–
WC6–30 1M	3.0	3.0
WC6–30 1M	3.1	3.1
WC6–30 1M	3.2	3.2
WC6–20 1M	3.5	3.5
WC6–20 1M	3.5	3.5
WC6–20 1M	3.6	3.6
WC6–10 1M	4.0	4.0
WC6–10 1M	4.2	4.2
WC6–10 1M	4.1	4.1
WC6	1.7	1.7
WC6	1.9	1.9
WC6	2.0	2.0

TABLE 7. Thickness, Microhardness, and Roughness of Electrospark-Deposited Composite Coatings on Steel 45 with Different Copper Contents of the Sublayer* in Electrospark Deposition

W_u, J	Cu weight increment, g/cm^2	Thickness, μm		Microhardness, GPa		R_a, μm
		layer	transition zone	layer	transition zone	
0.01	2.846	10–20	20	3.8–4.4	2.2–2.6	1.8
0.02	5.126	15–25	25	8.5–10.4	2.3–3.6	0.5
0.24	11.53	15–20	10	5.3–6.4	2.0–3.7	0.6
0.42	15.63	10–20	20	4.3–4.8	1.9–2.3	0.8
0.02*	2.317*	15–30	5–10	2.5; 11.5	3.3–4.3	2.4

* Copper coating was deposited as a second layer after WC8.

Multilayer Electrospark-Deposited Composite Coatings. We examined the formation of coatings on steel 45 samples preliminary covered with copper and then with hardmetal WC8 at discharge energy 0.42 J and T = = 1 min/cm^2. The data are provided in Table 7.

Our experiments show that greater spark discharge power increase the copper amount in the sublayer, decreases the aggregate microhardness of the surface layer, increases the roughness, and leads to the hardened layer 30–50 μm in thickness. The coating microhardness is quite high, to 10 GPa. Electrical erosion causes not only molten but also softened anode material to get into the gap between the electrodes under thermal and electrodynamic processes. Some part of the material emerged in the electrode gap reaches and interacts with the cathode [15]. Since copper more readily melts than the anode components, a mechanical mixture of copper with the anode material forms on the steel substrate; this explains a great scatter of microhardness in the surface layer. There is a copper film 1–2 μm in thickness on the coating, and all coatings formed in this way are of typical copper color (copper is revealed by X-rays on both the surface and inside the coating). With this sequence of the layers (Cu–WC8), the initially deposited copper coating melts when the WC–Co alloy is applied. Microirregularities and pores of the base coating are filled with the molten copper. The second layer crystallizes more slowly as heat is removed by the copper melt and surface roughness decreases to R_a = 0.5–0.9 μm.

For comparison, the composite coating was deposited in a reverse sequence, WC8–Cu, on one of the samples. In this case, the microhardness at a depth to 30 μm is 2.3–2.5 GPa. At a greater depth, there is a 5–10 μm thick layer with higher microhardness (8.0–12.3 GPa) and then a transition zone with microhardness 3.3–4.3 GPa. The regions with high microhardness on the coating are ridges of the previously deposited hardmetal WC8 coating. The roughness of the WC8–Cu coatings reaches 2.4 μm.

We also studied the properties of Ti, V, W, and WC composite coatings on steel 45. They were deposited in different sequences with Cu, In, Pb, Cd, and Sn sublayers (process sublayer at W_u = 0.02 J and T = 4–5 min/cm^2 and base material at 0.42 J and 1 min/cm^2). The experimental results are provided in Table 8. The thickness of the electrospark-deposited composite coating with the transition zone is 40–50 μm.

The composite coatings were deposited in the WC8–Cu–WC8 sequence. The first layer of hardmetal WC8 was applied in all cases at W_u = 0.4 J and the second (copper) and third (WC8) in different modes. The microhardness $H_μ$ of the surface layer is quite high (6.42–8.74 GPa) and its roughness is low (R_a = 0.5 μm) in all three coatings. There are no abrupt differences in the microhardness in the transition zone, the maximum microhardness on the surface smoothly decreasing with depth to reach that of the base metal. The optimum coating is produced when the first and third WC8 layers are deposited at W_u = 0.4 J and T = 1 min/cm^2, and copper at 0.24 J and 1.5 min/cm^2.

The experimental results have allowed a number of applied problems to be solved. For example, the technique for depositing Cu–WC8 and WC8–Cu–WC8 coatings and their further surface plastic rolling has already been used to restore engine rotor shaft necks, being bearing seats (Fig. 4*b*). The neck size was recovered (allowing for 0.4–0.5 mm polishing) employing electrospark deposition and rolling. The deposition of coatings and rolling

TABLE 8. Microhardness and Roughness of Electrospark-Deposited Composite Coatings

Coating material	Microhardness, GPa		Surface roughness R_a, μm
	layer	transition zone	
Uncoated steel 45	2.8	–	0.23
Ti	10.8, 9.6	3.7, 3.1	2.81
Ti–Cu	2.5, 9.5	3.6, 3.12	2.80
Cu–Ti	10.5	4.8, 3.7	0.90
V	8.5, 7.3	3.8, 3.3	3.19
V–Cu	2.3, 8.2	3.8, 3.3	2.80
Cu–V	8.4, 7.8	3.9, 3.3	0.80
W	9.5, 8.2	3.8, 3.4	3.26
W–Cu	2.5, 8.1	4.3, 3.6	3.14
Cu–W	9.5, 9.1	3.7, 3.2	0.65
WC	12.5, 11.0	4.7, 3.3	2.96
WC–Cu (1)	2.35, 12.3	4.19, 3.3	2.81
WC–Cu (2)	11.5, 10.49	4.76, 2.86	2.81
Cu–WC	12.3, 10.49	3.57, 3.3	0.48
In–WC	1.97, 2.5	3.86, 3.57	0.52
Pb–WC	2.6, 3.97	3.7, 3.3	0.56
Cd–WC	2.3, 3.8	3.6, 3.3	0.77
Sn–WC	2.0, 3.5	4.2, 3.1	0.59

alternated. A spring rod machine with a profile radius of 4 mm was used for rolling. The specific rolling force was 3000 MPa. This changed the residual stresses in the coating surface layer from tensile to compressive, decreased the coating surface roughness to R_a = 0.1 μm, and increased the fatigue strength wear resistance of the shaft [16]. The shaft neck maintenance and hardening technique has been introduced at the Uglegorsk and Mironovsky Power Stations, which involved arrangement of dedicated areas in maintenance shops.

CONCLUSIONS

Analysis of the microstructure and wear resistance of the alloys and kinetics of electrospark deposition using Ni–Cr–Al alloy electrodes has shown that the alloy from the ternary eutectic region (50.3 wt.% Ni, 40.2 Cr, and 9.5 wt.% Al) is the most effective for recovery of worn parts. The coatings produced with this alloy reach 1.0 mm in thickness.

The sintered 10–30 wt.% 1M (Ni–Cr–Si–B)–WC6 electrode materials allow the electrospark deposition of coatings with thickness to 100 μm and microhardness 12.3–14.2 GPa. The wear resistance and service life of these coatings are much greater than those produced with standard hardmetal WC6.

The layer-by-layer electrospark deposition of Cu, In, Pb, Cd, and Sn metals and Ti, V, and W metals, as well as their carbides and alloys of WC type onto metallic surfaces (provided that required process parameters are observed) increases the quality of the surface layer (compared to the coating without a sublayer): it combines adequate strength, lower roughness and porosity, and greater integrity.

The surface layer of WC8–Cu–WC8 coatings on steel substrates has microhardness in the range 6.42–8.74 GPa, smoothly decreasing with depth and reaching that of the base metal, and roughness R_a = 0.5 μm.

The experiments and actual experience show that the novel technique and new electrode materials can increase the resistance of cutting tools and service life of equipment parts by at least four times compared to uncoated ones and by two times compared to coated standard hardmetals of WC type.

REFERENCES

1. R. J. Wang, Y. Y. Qian, and J. Liu, "Structural and interfacial analysis of WC92–Co8 coating deposited on titanium alloy by electrospark deposition," *Appl. Surf. Sci.*, **228**, No. 4. – P. 405–409. 2004.
2. Yu. G. Tkachenko, D. Z. Yurchenko, V. F. Britun, et al., "Structure and properties of wear-resistant spark-deposited coatings produced with a titanium carbide alloy anode," *Powder Metall. Met. Ceram.*, **52**, No. 5–6, 306–313 (2013).
3. V. N. Gadalov, Yu. V. Boldyrev, and E. V. Ivanova, "Wear- and corrosion-resistant spark-deposited eutectic alloy coatings on steel 30KhGSA," *Uprochn. Tekhnol. Pokryt.*, No. 1, 22–25 (2006).
4. A. V. Paustovskii, Yu. G. Tkachenko, R. A. Alfintseva, et al., "Optimization of the composition, structure, and properties of electrode materials and spark-deposited coatings for strengthening and recovery of metallic surfaces," *Électron. Obrab. Mater.*, **49**, No. 1, 4–13 (2013).
5. M. S. Koval'chenko, Yu. G. Tkachenko, V. F. Britun, et al., "Structure, mechanical and erosive properties of AlN–$MoSi_2$ composite materials and their electrospark-deposited coatings," *Powder Metall. Met. Ceram.*, **47**, No. 3–4, 183–190 (2008).
6. I. A. Podchernyaeva, D. V. Yurechko, and A. D. Panasyuk, "Mass transfer and adhesion in electrospark alloying of AL9 alloy with AlN–Ti(Zr)B_2–Ti(Zr)Si_2 ceramic electrodes," *Powder Metall. Met. Ceram.*,. **43**, No. 9–10, 473–479 (2004).
7. Z. Chen and Y. Zhou, "Surface modification of resistance welding electrode by electro-spark deposited composite coatings. Part I: Coating characterization," *Surf. Coat. Technol.*, **201**, No. 3–4, 1503–1510 (2006).
8. I. A. Podchernyaeva, V. M. Panashenko, A. I. Dukhota, et al., "Formation and tribological behavior of multilayer wear-resistant ZrB_2-containing spark-deposited and spark-laser coatings on titanium alloy," *Probl. Tribol.*, No. 4, 96–101 (2012).
9. A. V. Paustovskii, Yu. G. Tkachenko, R. A. Alfintseva, et al., "Development of electrode materials for electrospark deposition and recovery of worn surfaces and structure and properties of coatings," *Électron. Obrab. Mater*., **47**, No. 2, 30–36 (2011).
10. A. N. Smirnov, V. K. Knyaz'kov, M. V. Radchenko, et al., "Effect of nanosized Al_2O_3 particles on structural and phase composition of Ni–Cr–B–Si–Fe/WC coatings produced by plasma powder welding," *Svarka Diagnos.*, No. 5, 32–37 (2012).
11. A. D. Pogrebnyak, S. N. Bratushka, V. V. Uglov, et al., "Structure and properties of Ni–Cr–B–Si–Fe/WC–Co coatings deposited on steel and copper substrates," *Fiz. Inzhen. Poverkhn.*, **6**, No. 1–2, 92–97 (2008).
12. L. A. Ivanov and G. P. Parkhomenko, "Sintered coatings for parts operating under erosive wear conditions," *Powder Metall. Met. Ceram.*, **13**, No. 2, 160–163 (1974).
13. V. B. Tarel'nik, "Improvement in the service properties of surface iron layers by application of composite electrospark coatings," *Électron. Obrab. Mater*., No. 4, 61–62 (1995).
14. V. B. Tarel'nik, *Quality Control of Surface Layers Applying Combined Electrospark Deposition* [in Russian], McDen, Sumy (2002), p. 323.
15. A. E. Gitlevich, V. V. Mikhailov, N. Ya. Parkanskii, and V. M. Revutskii, *Electrospark Deposition of Metallic Surfaces* [in Russian], Shtiintsa, Kishinev (1985), p. 196.
16. V. M. Leshchinskii and V. B. Tarel'nik, "Application of composite electrospark coatings with further plastic surface working," *Khim. Neft. Mashinostr.*, No. 3, 71–72 (1996).